Thermal annealing effect on spin coherence in ZnO single crystals

Z. Yang,[1,a),b)] Y. Li,[2] D. C. Look,[3] H. M. Zhou,[1] W. V. Chen,[4] R. K. Kawakami,[2] P. K. L. Yu,[4] and J. L. Liu[1,c)]

[1]*Quantum Structures Laboratory, Department of Electrical Engineering, University of California at Riverside, Riverside, California 92521, USA*
[2]*Department of Physics and Astronomy, University of California, Riverside, California 92521, USA*
[3]*Semiconductor Research Center, Wright State University, Dayton, Ohio 45435, USA*
[4]*Department of Electrical and Computer Engineering, University of California, San Diego, La Jolla, California 92093, USA*

(Received 21 November 2010; accepted 24 May 2011; published online 6 July 2011)

The spin coherence time (T_2^*) in ZnO single crystals at 8.5 K decreases significantly from ~11.2 ns to ~2.3 ns after annealing at 500 °C, as indicated by time-resolved Kerr-rotation pump-probe magneto-optical spectroscopy. The annealing-induced spin coherence degradation in ZnO arises neither from crystallinity degradation during the annealing process, as confirmed by x-ray rocking curves; nor from reflection variations of the probe laser beam induced by surface roughness changes during the annealing process, as confirmed by atomic force microscopy. Temperature-dependent Hall-effect studies indicate that decreased mobility and increased shallow-donor concentration in the annealing-induced surface conducting layer on top of the bulk ZnO are most likely to be the reasons for the spin coherence degradation in ZnO during the annealing process. © *2011 American Institute of Physics*. [doi:10.1063/1.3601869]

ZnO-based materials have great potential[1] in the areas of optoelectronics[2–5] and spintronics[6] because of a direct bandgap, large exciton binding energy,[1] and both theoretically predicted[7] and experimentally observed[8–10] above-room-temperature Curie temperature. For spintronic applications, spin coherence is a critically important parameter. Experimental studies of spin coherence in ZnO were first reported by Ghosh *et al.*[11] using time-resolved Faraday rotation (TRFR) pump-probe magneto-optical spectroscopy, with an observation of a spin coherence time as long as ~20 ns at $T = 30$ K in bulk ZnO samples. More recent experimental studies have shown an improvement in the spin coherence time in ZnO with an applied in-plane electric field confirmed by TRFR[12] and spin dynamics in ZnO quantum dots using TRFR[13]; theoretical works have studied mechanisms of spin dynamics in ZnO.[14,15] Many ZnO device applications, e.g., those requiring Ohmic contacts, involve an annealing step,[2–5,16] and it is not clear yet how spin coherence properties change during annealing. In this letter, spin coherence changes during annealing are reported and discussed.

Three identical high-quality ZnO single crystal samples kept un-annealed and annealed at 500 °C and 800 °C (for 2 min under N_2 ambient in a rapid-thermal-annealing oven) were employed in this study. The three samples are labeled as A-C, as shown in Table I. Time-resolved Kerr rotation (TRKR) pump-probe magneto-optical spectroscopy was employed to investigate the electron spin dynamics,[17] with ~360 nm wavelength used for both pump and probe laser sources, which matches ZnO bandgap (~3.437 eV at $T < 10$ K). Figure 1 shows the TRKR angle θ_K as a function of time delay Δt of samples A (top), B (middle), and C (bottom) measured at a temperature of 8.5 K and a magnetic field of $B = 90$ mT. The spin coherence times T_2^* of each sample shown in Fig. 1 are obtained by fitting $\theta_K \sim \Delta t$ relation using the equation

$$\theta_K(\Delta t) = A\cos(\omega_L \Delta t)\exp(-\Delta t/T_2^*). \tag{1}$$

The solid lines in Fig. 1 show the fitting curves. The other two fitting parameters, amplitude A and spin precession Larmor frequency ω_L, are summarized in Table I together with T_2^* for all three samples. The effective electron g-factor g^* of each sample is calculated using the equation

$$\omega_L = g^* \mu_B B/\hbar \tag{2}$$

and shown in Table I, where μ_B and $\hbar$ are Bohr magneton and Planck constant, respectively. The spin coherence time decreased from ~11.2 ns in sample A, to ~2.3 ns in sample B, and finally to ~2.0 ns in sample C, while g^* does not change much. The significantly decreased spin coherence time between unannealed ZnO (~11 ns) and annealed ZnO (~2 ns) samples indicates that additional spin scattering centers are formed during the annealing process. At elevated measurement temperatures, no analyzable spin coherence oscillation was obtained within the detection limit of the TRKR setup.

X-ray rocking curves (XRCs) were performed on the ZnO (0002) peaks (at $2\theta \sim 34.7°$, which dominates in the θ-2θ x-ray diffraction patterns[5]) to investigate the crystallinity[5,18] of samples A, B, and C, respectively, as shown with top, middle, and bottom curves in Fig. 2. The full-width-at-half-maximum (FWHM) of the XRC curves, obtained from

a)Electronic mail: zyang@seas.harvard.edu.
b)Present address: School of Engineering and Applied Sciences, Harvard University, Cambridge, MA 02138, USA.
c)Author to whom correspondence should be addressed. Electronic mail: jianlin@ee.ucr.edu.

 © 2011 American Institute of Physics

Author complimentary copy. Redistribution subject to AIP license or copyright, see http://jap.aip.org/jap/copyright.jsp

TABLE I. Sample preparations and spin-coherence parameters.

Sample	$t_{Annealing}$ (°C)	T_2^* (ns)	A (10^{-3} counts)	ω_L (GHz)	g^*
A	*un-annealed*	11.2	5.36	16.6	2.10
B	500	2.34	4.18	16.3	2.06
C	800	2.00	2.20	16.5	2.08

standard Gaussian fitting, decreases slightly from ~68 arc sec (sample A), to ~54 arc sec (sample B) and ~65 arc sec (sample C) after annealing. This indicates that the ZnO crystallinity does not degrade but actually improves slightly after annealing. Surface roughness may affect the reflection of the probe laser beam in TRKR measurements; however, atomic force microscopy (AFM) studies do not show any significant surface roughness changes in the annealed ZnO samples, with a root-mean-square roughness of ~1 nm for all three samples. The inset in Fig. 2 shows a 2-μm × 2-μm AFM image of sample A. So, neither crystallinity degradations nor surface roughness changes during annealing should be responsible for the spin coherence degradation in ZnO. In order to clarify the origin of the annealing-induced spin coherence degradation in ZnO, temperature-dependent Hall-effect measurements and two-layer fittings[17,19–21] were performed on the unannealed and annealed ZnO samples.

Figures 3(a) and 3(b) show the temperature dependence of the electron carrier concentration and mobility of samples A (squares), B (circles), and C (triangles) from 20 to 320 K. The symbols and the solid lines are the experimental data and theoretical fits, respectively. The fitting parameters are summarized in Table II. The most significant changes from sample A to B are those involving the surface conducting layer on top of the bulk layer: a thickness (d_{surf}) decrease (120 down to 19 nm), carrier concentration (n_{surf}) increase (2×10^{17} up to 1×10^{19} cm^{-3}), and mobility (μ_{surf}) decrease (1000 down to 230 cm^{2}V^{-1}s^{-1}). Much smaller changes occur in the bulk donor and acceptor concentrations. The laser penetration depth in ZnO is around 60–100 nm.[22,23] For sample A, the laser absorption is mostly in the surface layer (120 nm), but the surface layer of sample A is of better "quality" than the surface layers of the annealed samples,

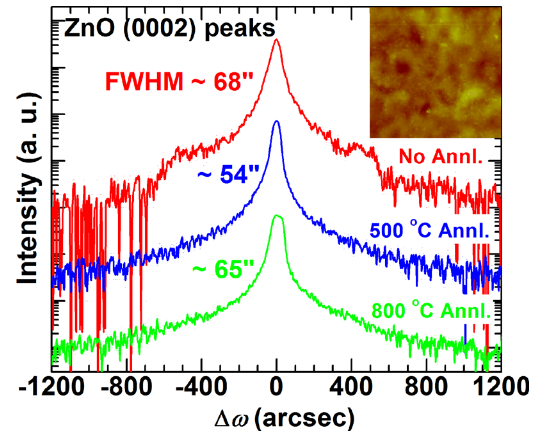

FIG. 2. (Color online) X-ray rocking curves of the ZnO (0002) peaks from samples A (top), B (middle), and C (bottom) measured at room temperature with FWHMs of ~68, ~54, and ~65 arc sec, respectively. The inset shows the AFM image of sample A within a 2 μm × 2 μm area.

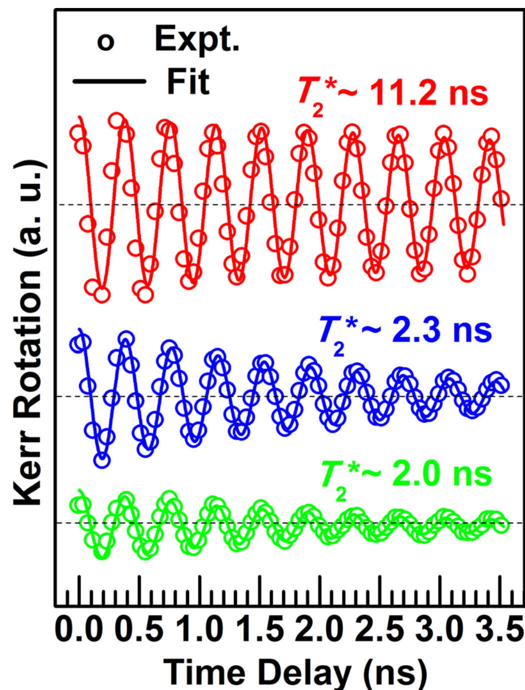

FIG. 1. (Color online) Time-resolved Kerr rotation of samples A (top), B (middle), and C (bottom) measured at 8.5 K and 90 mT. The circles and the solid lines represent experimental data and theoretical fits, respectively. The spin coherence time T_2^* obtained from fitting is ~11.2, ~2.3, and ~2.0 ns for samples A, B, and C, respectively. The curves are vertically shifted for clarity and the black dashed lines show the zeros of each curve.

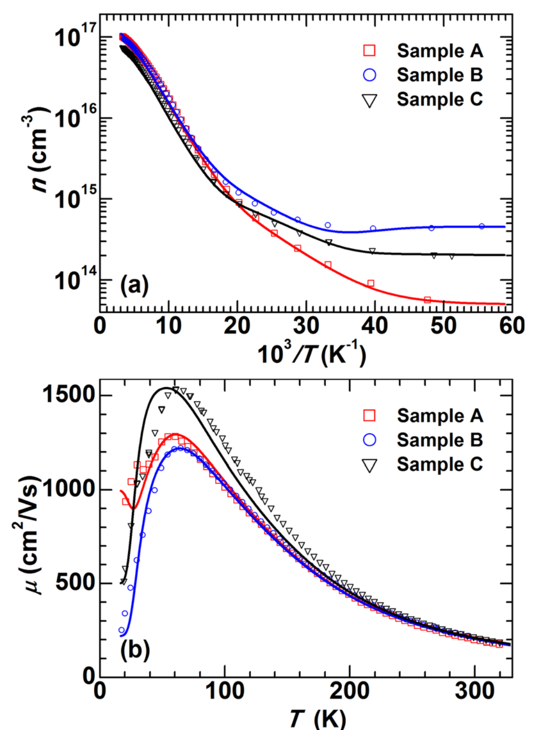

FIG. 3. (Color online) Temperature-dependent (20-320 K) electron carrier concentration (a) and Hall mobility (b) of samples A (squares), B (circles), and C (triangles). The solid lines are the theoretical fits.

Author complimentary copy. Redistribution subject to AIP license or copyright, see http://jap.aip.org/jap/copyright.jsp

TABLE II. Fitting parameters of the temperature-dependent Hall-effect analyses.

Sample	E_{D1} (meV)	N_{D1} (10^{17} cm^{-3})	E_{D2} (meV)	N_{D2} (10^{15} cm^{-3})	N_A (10^{15} cm^{-3})	μ_{surf} (cm^2/Vs)	n_{surf} (10^{17} cm^{-3})	d_{surf} (nm)
A	47	1.3	12	7.4	6.4	1000	2	120
B	47	1.3	12	9.2	7.2	230	100	19
C	51	0.9	12	4.4	3.4	506	10	87

with a mobility of $\sim$1000 cm^2/Vs, and a relatively low total surface concentration $n_{s,surf} = n_{surf} \times d_{surf} = 2.4 \times 10^{12}$ cm^{-2}. In sample B, the surface scattering is much stronger, since the mobility is much smaller, and the sheet carrier density, $n_{s,surf} = 1.9 \times 10^{13}$ cm^{-2}, is much larger, even though the surface layer is thinner. From the above analyses, we conclude that these changes in the surface layer may be responsible for the significantly decreased spin coherence time in ZnO after 500 °C-annealing. The spin coherence difference between samples B and C ($\sim$2.3 versus $\sim$2.0 ns) is small comparing to that between samples A and B ($\sim$11.2 versus $\sim$2.3 ns). In sample C, $n_{s,surf} = 8.7 \times 10^{12}$ cm^{-2}, which is also larger than in sample A, and based on a simple comparison of $n_{s,surf}$ values alone, sample C should have a longer T_2^* than that of sample B. However, it also may be important that d_{surf} is larger in sample C than in sample B, and, thus, the spins spend more time in the relatively poor surface region. The slightly poorer crystallinity of sample C than B may also contribute to the small difference in T_2^*. Based on the PL analyses,[17] the donor state N_{D1} in Table II is associated with hydrogen (H) and group-III elements (Al/Ga/In),[21,24] while the acceptor state N_A is possibly due to Zn vacancies.[17,25–27] Loss of H after annealing is observed for the dominating PL peak red shifts, which is commonly observed in ZnO samples annealed at temperatures above 500 °C.[21] The reason of formation of surface conducting layer on top of the bulk ZnO with decreased mobility and increased shallow-donor concentration after annealing is most likely to be the surface accumulation of group-III elements (Al/Ga/In) during annealing, indicated by PL spectra, which is consistent with previous secondary-ion mass spectroscopy studies.[20] The possible dominating spin de-coherence mechanisms were discussed in the supporting materials (ref. 17).

In summary, time-resolved-Kerr-rotation pump-probe magneto-optical spectroscopy was employed to investigate the spin dynamics in ZnO single crystal samples before and after annealing. It is observed that the spin coherence time (T_2^*) in unannealed ZnO sample is as long as $\sim$11.2 ns at 8.5 K, but significantly decreases to $\sim$2.3 ns after 500 °C annealing. X-ray rocking curves and atomic force microscopy confirm that the crystallinity and surface roughness do not change appreciably during annealing and, thus, are not responsible for the spin-coherence degradation. Temperature-dependent Hall effect measurements indicate that the annealing-induced spin coherence degradation is likely due to decreased mobility and increased carrier concentration in the thin conducting layer on the surface of the bulk ZnO.

This work was supported by ONR/DMEA (H94003-08-2-0803) through the Center for Nanomaterials and Nanodevices (CNN). The work of DCL was supported by AFOSR Grant FA9550-10-1-0079 (K. Reinhardt) and NSF Grant DMR0803276 (L. Hess).

[1] D. C. Look, Mater. Sci. Eng., B **80**, 383 (2001).
[2] J. Kong, S. Chu, M. Olmedo, L. Li, Z. Yang, and J. L. Liu, Appl. Phys. Lett. **93**, 132113 (2008).
[3] S. Chu, M. Olmedo, Z. Yang, J. Y. Kong, and J. L. Liu, Appl. Phys. Lett. **93**, 181106 (2008).
[4] L. Li, Z. Yang, J. Y. Kong, and J. L. Liu, Appl. Phys. Lett. **95**, 232117 (2009).
[5] Z. Yang, S. Chu, W. V. Chen, L. Li, J. Kong, J. Ren, P. K. L. Yu, and J. Liu, Appl. Phys. Express **3**, 032101 (2010).
[6] C. Liu, F. Yun, and H. Morkoç, J. Mater. Sci.: Mater. Electron. **16**, 555 (2005).
[7] T. Dietl, H. Ohno, F. Matsukura, J. Cibert, and D. Ferrand, Science **287**, 1019 (2000).
[8] Z. Yang, J. L. Liu, M. Biasini, and W. P. Beyermann, Appl. Phys. Lett. **92**, 042111 (2008).
[9] Z. Yang, M. Biasini, W. P. Beyermann, M. B. Katz, O. K. Ezekoye, X. Q. Pan, Y. Pu, J. Shi, Z. Zuo, and J. L. Liu, J. Appl. Phys. **104**, 113712 (2008).
[10] Z. Yang, W. P. Beyermann, M. B. Katz, O. K. Ezekoye, Z. Zuo, Y. Pu, J. Shi, X. Q. Pan, and J. L. Liu, J. Appl. Phys. **105**, 053708 (2009).
[11] S. Ghosh, V. Sih, W. H. Lau, D. D. Awschalom, S.-Y. Bae, S. Wang, S. Vaidya, and G. Chapline, Appl. Phys. Lett. **86**, 232507 (2005).
[12] S. Ghosh, D. W. Steuerman, B. Maertz, K. Ohtani, H. Xu, H. Ohno, and D. D. Awschalom, Appl. Phys. Lett. **92**, 162109 (2008).
[13] N. Janβen, K. M. Whitaker, D. R. Gamelin, and R. Bratschitsch, Nano Lett. **8**, 1991 (2008).
[14] N. J. Harmon, W. O. Putikka, and R. Joynt, Phys. Rev. B **79**, 115204 (2009).
[15] J. Tribollet, Eur. Phys. J. B **72**, 531 (2009).
[16] L. J. Mandalapu, Z. Yang, and J. L. Liu, Appl. Phys. Lett. **90**, 252103 (2007).
[17] See supplemental materials at http://dx.doi.org/10.1063/1.3601869 for experimental details and supplemental discussions.
[18] Z. Yang, H. M. Zhou, W. V. Chen, L. Li, J. Z. Zhao, P. K. L. Yu, and J. L. Liu, J. Appl. Phys. **108**, 066101 (2010).
[19] D. C. Look, J. Appl. Phys. **104**, 063718 (2008).
[20] D. C. Look, B. Claflin, and H. E. Smith, Appl. Phys. Lett. **92**, 122108 (2008).
[21] D. C. Look, G. C. Farlow, P. Reunchan, S. Limpijumnong, S. B. Zhang, and K. Nordlund, Phys. Rev. Lett. **95**, 225502 (2005).
[22] V. Srikant and D. R. Clarke, J. Appl. Phys. **81**, 6357 (1997).
[23] J. F. Muth, R. M. Kolbas, A. K. Sharma, S. Oktyabrsky, and J. Narayan, J. Appl. Phys. **85**, 7884 (1999).
[24] B. K. Meyer, H. Alves, D. M. Hofmann, W. Kriegseis, D. Forster, F. Bertram, J. Christen, A. Hoffmann, M. Straßburg, M. Dworzak, U. Haboeck, and A. V. Rodina, Phys. Status Solidi B **241**, 231 (2004).
[25] Z. Yang, D. C. Look, and J. L. Liu, Appl. Phys. Lett. **94**, 072101 (2009).
[26] Z. Yang and J. L. Liu, J. Vac. Sci. Technol. B **28**, C3D6 (2010).
[27] F. Tuomisto, V. Ranki, K. Saarinen, and D. C. Look, Phys. Rev. Lett. **91**, 205502 (2003).

Author complimentary copy. Redistribution subject to AIP license or copyright, see http://jap.aip.org/jap/copyright.jsp